the FEBS Journal

Biosynthesis of UDP-glucuronic acid and UDP-galacturonic acid in *Bacillus cereus* subsp. cytotoxis NVH 391-98

Bryan Broach[1,*], Xiaogang Gu[1,*] and Maor Bar-Peled[1,2]

1 Complex Carbohydrate Research Center (CCRC), University of Georgia, Athens, GA, USA
2 Department of Plant Biology, University of Georgia, Athens, GA, USA

Keywords
alkalinity; *Bacillus*; biofilm; UDP-galacturonic acid; UDP-glucuronic acid

Correspondence
M. Bar-Peled, CCRC, 315 Riverbend Road, Athens, GA 30602, USA
Fax: +1 706 542 4412
Tel: +1 706 542 2062
E-mail: peled@ccrc.uga.edu

*These authors contributed equally to this work

(Received 21 June 2011, revised 15 September 2011, accepted 10 October 2011)

doi:10.1111/j.1742-4658.2011.08402.x

The food borne pathogen *Bacillus cereus* produces uronic acid-containing glycans that are secreted in a shielding biofilm environment, and certain alkaliphilic *Bacillus* deposit uronate-glycan polymers in the cell wall when adapting to alkaline environments. The source of these acidic sugars is unknown and, in the present study, we describe the functional identification of an operon in *Bacillus cerues* subsp. cytotoxis NVH 391-98 that comprises genes involved in the synthesis of UDP-uronic acids in *Bacillus* spp. Within the operon, a UDP-glucose 6-dehydrogenase converts UDP-glucose in the presence of NAD^+ to UDP-glucuronic acid and NADH, and a UDP-GlcA 4-epimerase (UGlcAE) converts UDP-glucuronic acid to UDP-galacturonic acid. Interestingly, *in vitro*, both enzymes can utilize the TDP-sugar forms as well, albeit at lower catalytic efficiency. Unlike most of the very few bacterial 4-epimerases that have been characterized, which are promiscuous, the *B. cereus* UGlcAE enzyme is very specific and cannot use UDP-glucose, UDP-*N*-acetylglucosamine, UDP-*N*-acetylglucosaminuronic acid or UDP-xylose as substrates. Size exclusion chromatography suggests that UGlcAE is active as a monomer, unlike the dimeric form of plant enzymes; the *Bacillus* UDP-glucose 6-dehydrogenase is also found as a monomer. Phylogenic analysis further suggests that the *Bacillus* UGlcAE may have evolved separately from other bacterial and plant epimerases. Our results provide insight into the formation and function of uronic acid-containing glycans in the lifecycle of *B. cereus* and related species containing homologous operons, as well as a basis for determining the importance of these acidic glycans. We also discuss the ability to target UGlcAE as a drug candidate.

Database
- Nucleotide sequence data have been deposited in the Genbank database with the accession numbers HM581979 and HM581980.

Introduction

Bacillus cereus has garnered much notoriety as a food-poisoning bacterium and, similar to its close relatives, the human pathogen *Bacillus anthracis* and the insecticidal *Bacillus thuringiensis*, *B. cereus* has several life forms. For example, it can survive as a protective endospore in harsh conditions, in a shielding biofilm

Abbreviations
Gal, galactose; GalA, galacturonic acid; Glc, glucose; GlcA, glucuronic acid; GlcNAc, *N*-acetylglucosamine; GlcNAcA, *N*-acetylglucosaminuronic acid; Rha, rhamnose; UGlcAE, UDP-glucuronic acid 4-epimerase; UGlcDH, UDP-glucose 6-dehydrogenase.

environment, or as a free-living cell in soil and water. An explanation of how changes in surface glycans confer advantages to *Bacillus* species during different stages of its life cycle is of great interest for understanding the pathogenesis of the organism. However, as a result of the infectious nature *B. cereus* and related *Bacillus* spp., it is understandable that many glycans have yet to be characterized, particularly those that may be made by the pathogen within the human body. Recently, polysaccharides isolated from spores of *B. anthracis* were shown to be antigenic and similar to cross-reactive epitopes found only in pathogenic strains of *B. cereus*, highlighting the role of carbohydrates in *Bacillus* spp. infections [1]. To identify new metabolic pathways involved in the formation of surface glycans in these pathogens, we aimed to identify putative genes encoding enzymes involved in the synthesis of glycan precursors (i.e. nucleotide sugars). These nucleotide sugars are used by specific glycosyltransferases to make the different polysaccharide structures in an organism.

The occurrence of the sugar residue galacturonic acid (GalA) in cell surface glycans varies across different bacterial species. In Gram-negative bacteria, for example, the amount and distribution of GalA in lipopolysaccharides, the major glycan molecule in the outer cell surface membrane [2], shows significant variations. For example, the core oligosaccharide portion of the lipopolysaccharides in the symbiotic nitrogen-fixing bacteria *Rhizobium leguminosarum* [3] and *Bradyrhizobium japonicum* [4], and in the pathogen *Klebsiella pneumonia* [5], consists of several GalA residues. However, the core oligosaccharides of *Escherichia coli* and *Salmonella typhimurium* lack GalA and, instead, consist of glucosamine residues. One reason for the variations in surface glycans could be that organisms form specific glycans to facilitate exclusive interactions with a particular host. Alternatively, specific glycans may display a mimicry-like structure to facilitate entry into the host, or perhaps to allow the bacteria to survive under different environmental conditions. It is also a possibility that the negative charge of acidic sugars (glycuronosyl residues) functions as an ionic barrier or to sequester metals required for normal organism function.

GalA-containing glycans have also been reported in Gram-positive bacteria. For example, GalA has been observed in the capsule of *Streptococcus pneumoniae* serotype 1 [6]. Interestingly, the bacterial capsular surface in *S. pneumoniae* was suggested to comprise the first barrier against the innate immune system, as well as being involved in mediating attachment to cells/surfaces to resist clearance. Recent analyses of *B. cereus* growing in biofilm have indicated that it secretes exopolysaccharides consisting of the glycuronosyl residues glucuronic acid (GlcA) and GalA [7]. GlcA and GalA residues, however, were not reported in *B. cereus* glycans isolated from spores or cultures grown in the laboratory [8–10].

Synthesis of UDP-galacturonic acid (UDP-GalA) [11,12] has been studied extensively in plants, where UDP-glucose (UDP-Glc) is first converted to UDP-glucuronic acid (UDP-GlcA) by UDP-glucose 6-dehydrogenase (annotated as UGDH, UGD, UDP-GlcDH or UGlcDH). Subsequently, a very specific membrane-bound 4-epimerase, UDP-GlcA 4-epimerase (UGlcAE) [13,14] interconverts UDP-GlcA and UDP-GalA. Fewer bacterial UGlcAEs have been characterized, and questions still remain concerning how the specificity for UDP-GlcA of these epimerases varies across bacterial species. Studies of the *Streptococcus pneumococcus* type I epimerase [15] and Gla_{kp} from *Klebsiella pneumoniae* have shown that the enzymes are capable of interconverting several UDP-sugars, including UDP-GlcA, UDP-Glc and UDP-*N*-acetylglucosamine (GlcNAc) [5]. On the other hand, the characterization of the type I *S. pneumococcus* Cap1J 4-epimerase demonstrated that the enzyme had specificity for the uronic acid moiety because it was unable to interconvert UDP-Glc or UDP-Gal [16]. In the present study, we report the identification and characterization of two genes (*BcUGlcDH* and *BcUGlcAE*) involved in the biosynthesis of UDP-GlcA and UDP-GalA (Fig. 1A) from *Bacillus cereus* subsp. cytotoxis NVH 391-98. Interestingly, the operon for these two genes is not common in all *Bacillus* spp., which may provide insight into the roles of these charged-glycans within the life-cycle of this pathogen.

Results

Bioinformatic analyses of UGlcDH and UGlcAE in *Bacillus*

A BLAST analysis with characterized proteins from plants and bacteria was performed to identify enzymes involved in UDP-GalA production in *B. cereus*; and those with the greatest homology to known UGlcAE and UGlcDH were selected for further study. However, the validation of the selected enzymes based on the homology alone was challenging as a result of relative low amino-acid sequence identity with the known enzymes. For example, the potential dehydrogenase from *B. cereus*, Bcer98_2076, shares only 35%, 32%, 31% and 32% amino-sequence identity with functional UGlcAE from *Drosophila* (sugarless, UDP-Glc

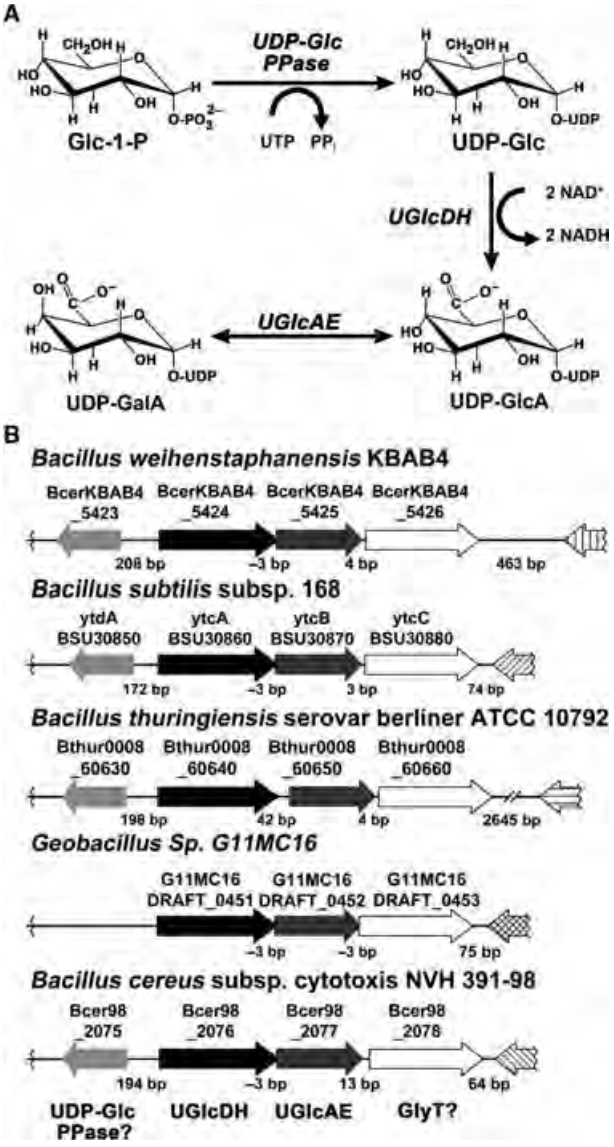

Fig. 1. The biosyntheses of acidic sugar nucleotides in *Bacillus*. (A) In *Bacillus*, based on the present report, UDP-Glc pyrophosphorylase (UDP-Glc PPase) converts Glc-1-P and UTP to UDP-Glc. In the presence of NAD^+, UDP-Glc is interconverted by UDP-glucose dehydrogenase (UGlcDH) into UDP-GlcA and NADH. UDP-GlcA can then be interconverted by the 4-epimerase, UGlcAE, into UDP-GalA. (B) Organization of the three genes within the UGalA operon and the flanking regions across selective members of *Bacillus* spp. The locus number for each gene in the operon across the different species shown is indicated. Based on this report, Bcer98_2076 functions as a UGlcDH and Bcer98_2077 as a UGlcAE. The operon also comprises a putative glycosyltransferase (Bcer98_2078 in *B. cereus*), which may be involved in the synthesis of GlcA or GalA-containing glycans. Note: except for *Geobacillus* sp. G11MC16, in the 5′ region flanking the UGalA operon, there is a single gene in the opposite direction of the operon encoding a putative UDP-Glc PPase (Bcer98_2075 in *B. cereus*, putative ytdA in *B. subtilis*).

dehydrogenase), plants (AtUGlcDH), *Cryptococcus* (Ugd1) and Gram-negative *Sinorizobium* (rkpK, SMc02641), respectively (Fig. S1A). In addition, the Bcer98_2076 also shares 38% sequence identity with functional GDP-mannose dehydrogenase from *Pseudomonas aeruginosa* [17]. Similarly, the potential epimerase from *B. cereus*, Bcer98_2077, shares 36% and 32% sequence identity with functional UGlcAE (AtUGlcAE3) from plants, and LpsL from *Sinorizobium* (SMc02640), respectively (Fig. S2B). Having such relative low sequence identities, it is impossible to predict the function for these putative *Bacillus* spp. UGlcDH and UGlcAE homologs without further biochemical characterization. Interestingly, the putative dehydrogenase, Bcer98_2076, and epimerase, Bcer98_2077, from *B. cereus* are found in the same operon along with a putative glycosyltransferase, Bcer98_2078, that shares sequence similarity to an annotated lipopolysaccharide *N*-acetylglucosaminyltransferase. Similar operons (Fig. 1B) with homologous genes are found in *Bacillus subtilis* subsp. 168, *Bacillus weihenstephanensis* KBAB4, *Bacillus thuringiensis* serovar berliner ATCC 10792 and *Geobacillus* sp. G11MC16, whereas such operon organization is not found in the genomes of other *Bacillaceae*, such as *B. anthracis* strains Ames, A0248 or CDC 684. A putative nucleotidyl transferase, Bcer98_2075, is also found in proximity to the operon containing the putative dehydrogenase and epimerase, and homologous genes are found alongside the operon in *B. subtilis* subsp. 168, *B. weihenstephanensis* KBAB4, and *B. thuringiensis* serovar berliner ATCC 10792 but absent from *Geobacillus* sp. G11MC16. In *B. subtilis* subsp. 168, the homologous gene (ytdA BSU30850) is annotated as a putative UDP-glucose pyrophosphorylase, suggesting that Bcer98_2075 and its homologs may play a role in the synthesis of UDP-Glc (Fig. 1A) for subsequent interconversion to UDP-GlcA and UDP-GalA. To determine and elaborate upon the functions of the putative *B. cereus* UGlcDH and UGlcAE, we have cloned and expressed the genes as recombinant proteins in *E. coli* and examined their enzyme activities.

Biochemical characterization of *B. cereus* UGlcDH and UGlcAE

A distinct protein band migrating slightly lower than the 50 kDa standard, was detected by SDS/PAGE analysis of the extracts from *E. coli* cells expressing recombinant BcUGlcDH (Fig. 2A, lane 2) but was absent in *E. coli* cells expressing the control vector. The expressed UGlcDH protein (theoretical mass 49,792) was purified (Fig. 2A, lane 4) and shown,

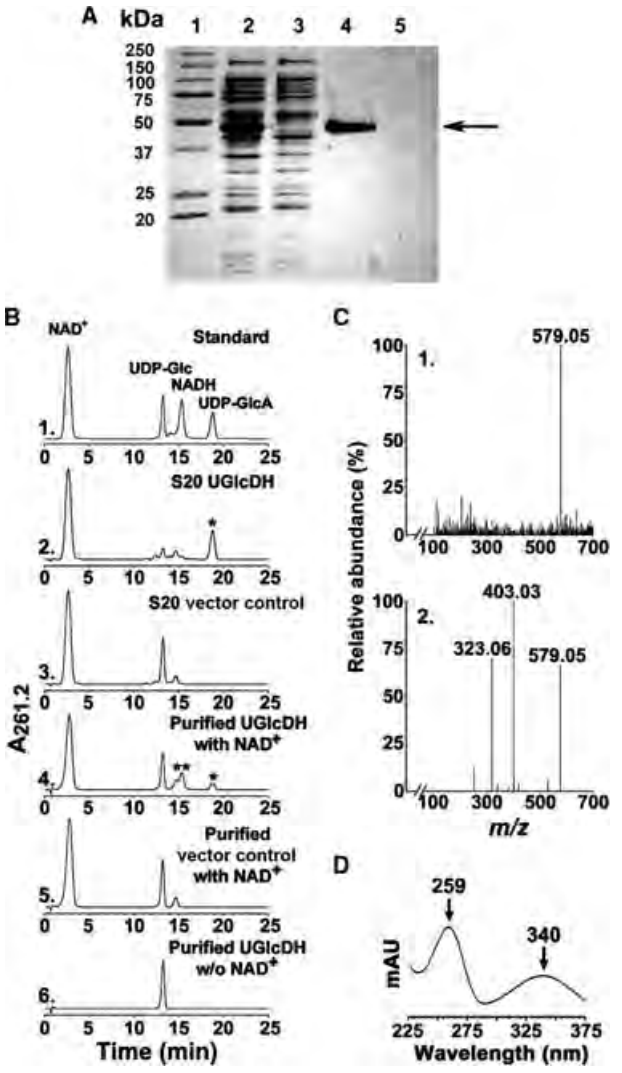

Fig. 2. Expression and characterization of recombinant of BcUGlcDH. (A) SDS/PAGE of total soluble protein isolated from *E. coli* cells expressing UGlcDH (lane 2), negative vector control (lane 3) and of column-purified UGlcDH or control (lanes 4 and 5, respectively). An arrow points to the purified protein. (B) High-performance anion-exchange chromatography of the products formed by UGlcDH. Purified recombinant UGlcDH was reacted with UDP-Glc for 30 min in the presence (panel 4) or absence (panel 6) of NAD^+. The corresponding column-purified protein isolated from cells expressing the control vector was reacted with UDP-Glc and NAD^+ for 30 min (panel 5) as a control. The reaction products were separated on a Q15 anion-exchange column. The distinct UDP-sugar peak marked by an asterisk (panels 2 and 4 with a retention time of 18.8 min) was collected and characterized by mass spectrometry and ^{1}H-NMR spectroscopy. The activity of total soluble protein (denoted S20) isolated from cells expressing recombinant BcUGlcDH (panel 2) or vector control (panel 3) is also shown. (C) Analysis of BcUGlcDH enzymatic product by MS operated in the negative ion mode. The HPLC peak (panel 2B or 4B, *) was collected and directly infused to ESI-MS. The spectrum of the full MS molecular ions (panel 1, *m/z* of 579.05 for deprotonated $[M\text{-}H]^-$) and of the derived CID-fragments (panel 2, *m/z* of 323.06 and 403.05) are shown. (D) The peak in panel 4B marked by a double asterisk (**) has major UV absorbance peaks at 259 and 340 nm, the characteristic absorbance signature for NADH.

using a HPLC-based assay, to convert UDP-Glc to a new UDP-sugar (Fig. 2B, panels 2 and 4, asterisk) in the presence of NAD^+ and to a product that migrated as NADH (Fig. 2B, panel 4, double asterisk) with a characteristic dual UV absorption maximum at 259 and 340 nm (Fig. 2D). The newly formed UDP-sugar eluted from the Q15 ion-exchange column with a retention time (18.8 min), comparable to UDP-GlcA standard (Fig. 2B, panel 1). Analysis of the reaction product peak by ESI-MS operated in the negative ion mode identified an ion product (Fig. 2C, panel 1) of *m/z* 579.05, as expected for a UDP-hexuronic acid. Collision-induced ion fragmentation yielded two major ions at *m/z* 323.06 and 403.03 (Fig. 2C, panel 2), suggesting the formation of UMP and UDP ions, as expected. The dehydrogenase enzymatic reaction was also followed with ^{1}H-NMR (Fig. 3). As time advanced during the real-time NMR assay, a clear decrease of the peak corresponding to the anomeric proton (peak G1″, 5.62 p.p.m.) of UDP-Glc was observed alongside a simultaneous increase of the peaks corresponding to the anomeric and H-5″ protons of UDP-GlcA (peaks A1″ and A5″, 5.64 and 4.16 p.p.m., respectively). Additionally, the signal from the protons added to the NAD^+ nicotinamide ring after enzymatic reduction to NADH (peak H1a,b) appeared in the spectrum in the range 2.7–2.9 p.p.m. as time advanced. Peaks from other diagnostic protons of NAD^+ (N3, N5, N6, N7) were also diminished concomitantly with an increase of diagnostic peaks of NADH (H2, H3, H4a,b, H5, H6, H7). The ratio of the change in the diagnostic NADH proton signals compared to those of UDP-GlcA was found to be 2 : 1, validating that two moles of NAD^+ are reduced per mole of UDP-GlcA made in the enzymatic reaction. Hence, we named Bcer98_2076 as UDP-Glc 6-dehydrogenase (i.e. UGlcDH, or dehydrogenase).

To determine substrate specificity, other nucleotide-glucose were tested. TDP-Glc was a substrate for the dehydrogenase as well, albeit with lower efficiency compared to UDP-Glc (Table 1). The dehydrogenase, however, could not utilize ADP-Glc, GDP-Glc or GDP-mannose as substrates. In addition, $NADP^+$ could not substitute NAD^+ as the cofactor. After the reaction with TDP-Glc, the enzyme product was validated as TDP-GlcA as determined by MALDI-TOF

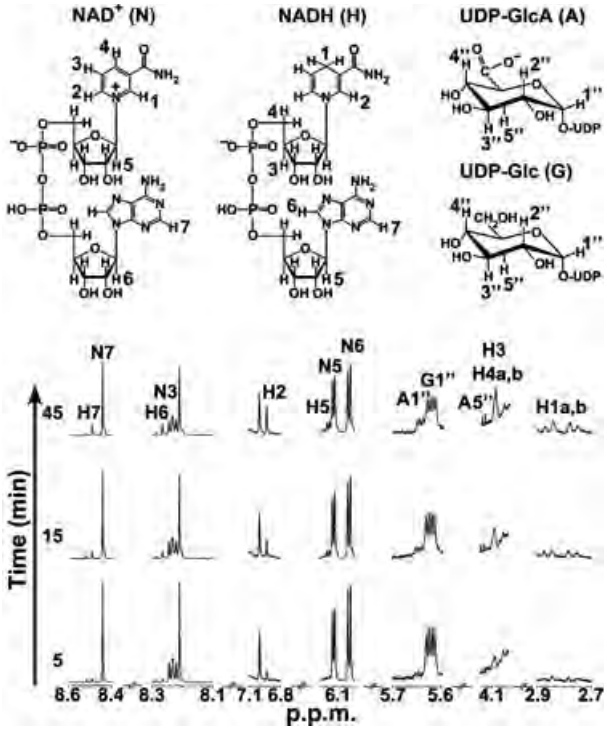

Fig. 3. Analysis of BcUGlcDH enzymatic reaction in time-resolved ^{1}H-NMR. Selected regions of the 600 mHz ^{1}H-NMR spectrum show the interconversion of UDP-α-D-Glc and NAD^+ to UDP-α-D-GlcA and NADH at 5, 15 and 45 min after the reaction was initiated. Diagnostic peaks of NAD^+ and NADH are labeled N and H, respectively, whereas UDP-Glc peaks are labeled G and UDP-GlcA peaks are labeled A. Peaks are arbitrarily numbered to denote corresponding protons numbered as indicated in the molecular structures.

Table 1. Steady-state kinetics parameters of recombinant BcUGlcAE and BcUGlcDH. Kinetics of UGlcAE were measured with varied concentrations of UDP-GlcA (0.1–1.0 mM) or TDP-GlcA (0.08–0.5 mM) and 1 mM NAD^+ after 8 min at standard conditions. The reciprocal initial velocity was plotted against the reciprocal UDP-GlcA or TDP-GlcA concentration according to Lineweaver and Burk to calculate the corresponding K_m values. The data presented are the mean K_m values from three experiments. Kinetics of BcUGlcDH were measured with 2 mM NAD^+ and varied concentrations of UDP-Glc (0.1–1.0 mM) after 15 min or with varied concentrations of TDP-Glc (0.1–1.0 mM) after 25 min under standard conditions. Kinetics of BcUGlcDH were also measured with varied concentrations of NAD^+ (0.1–2 mM) with 1 mM UDP-Glc after 15 min or 1 mM TDP-Glc after 25 min under standard conditions. The data presented are the average K_m values from two experiments.

	K_m (mM)	k_{cat} (s^{-1})	k_{cat}/K_m ($mM^{-1}\cdot s^{-1}$)
UDP-GlcAE activity	0.12 ± 0.01	3.2 ± 0.1	26 ± 1.4
TDP-GlcAE activity	0.18 ± 0.01	2.1 ± 0.1	12 ± 0.4
UDP-GlcDH activity – (UDP-Glc)	0.137 ± 0.019	0.974 ± 0.031	7.1 ± 1.0
UDP-GlcDH activity – (NAD^+)	0.042 ± 0.006	0.898 ± 0.014	21.4 ± 3.1
TDP-GlcDH activity – (TDP-Glc)[a]	2.07 ± 0.39	0.646 ± 0.091	0.31 ± 0.073
TDP-GlcDH activity – (NAD^+)	0.664 ± 0.050	0.307 ± 0.012	0.46 ± 0.039

[a] The kinetic values for TDP-Glc and NAD are an estimate and likely qualitative rather than quantitative because the reaction with TDP-Glc could not be carried out at saturation. This in turn may affect the K_{cat} value for NAD. Nonetheless, the data provide sufficient information showing that the dehydrogenase is more efficient with UDP-Glc as the substrate.

MS in the negative mode with a major *m/z* ion at 577.6 and by ^{1}H-NMR (Fig. 4A,B). To determine the preferred *in vivo* substrate of dehydrogenase, *E. coli* harboring the expression plasmid was grown to mid-log phase and, 2 h after induction, the cells were extracted and the amount of UDP-sugar produced by *E. coli* determined by HPLC and ESI-MS/MS. HPLC analyses reveal a major peak at 18.3 min (comparable to the UDP-GlcA standard peak) that is absent from NDP-sugars extracted from *E. coli* control (data not shown). MS analyses confirm the *in vivo* production of UDP-GlcA as the major ion as well. Interestingly, *in vitro* the dehydrogenase was unable to fully convert UDP-Glc to UDP-GlcA; this was later confirmed (see below) as a result of strong inhibition of the enzyme by its product NADH.

We next proceeded to characterize the function of the second gene in the operon, Bcer98_2077. Expression of this recombinant protein in *E. coli* yielded a highly expressed protein migrating alongside a 37 kDa marker as expected from the theoretical mass (36 734) (Fig. 5A, lane 3). The enzyme was tested against various commercially available ADP-, UDP- and GDP-sugars in the presence or absence of co-factors. The recombinant Bcer98_2077 converted a portion of UDP-GlcA to a new peak migrating at 22.5 min when separated on the HPLC column (Fig. 5B, panels 2 and 3, arrow). The peak was collected from the column and ^{1}H-NMR confirmed the enzyme product as UDP-GalA because it had identical proton assignments as described previously [14]. Thus, the enzyme is a true 4-epimerase because it is capable of interconverting UDP-GalA to UDP-GlcA (not shown) as well. Hence, we named Bcer98_2077 as UDP-GlcA 4-epimerase, BcUGlcAE. Based on the sensitivity of our assay, this *B. cereus* 4-epimerase was unable to convert UDP-glucose or UDP-xylose. The characterization of a 4-epimerase in *P. aeruginosa* capable of epimerizing UDP-GlcNAc and UDP-GlcNacA [18] and the recent identification of a UDP-GlcNAc 6-dehydrogenase in

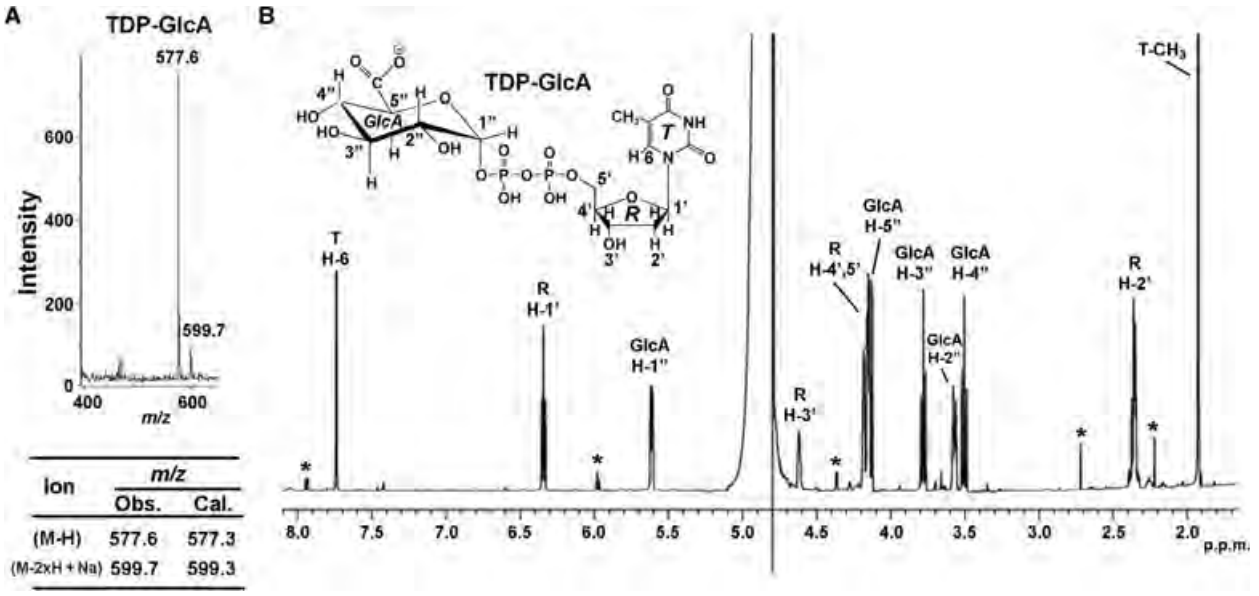

Fig. 4. BcUGlcDH can convert TDP-Glc to TDP-GlcA as determined by MALDI and NMR. (A) MALDI-MS analysis: negative-ion MALDI mass spectra were recorded using a Microflex LT mass spectrometer (Bruker Daltonik, Bremen, Germany). Aqueous samples (1 μL) of 1 mM TDP-GlcA (produced from the dehydrogenase reaction with TDP-Glc/NAD^+ and collected by HPLC) were mixed with an equal volume of matrix solution (1 $\mu g \cdot \mu L^{-1}$ 2,5-dihydroxybenzoic acid in 50% methanol) and dried on the plate. Spectra from 500 laser (N_2; 337 nm) shots were summed to generate a mass spectrum. The ion mass, calculated (abbr. Cal.) or observed (abbr. Obs.), are listed below the spectrum. (B) ^{1}H-NMR spectroscopy at 600 MHz of the HPLC collected peak after reaction of BcUGlcDH with TDP-Glc and NAD^+. The assignments of each proton are indicated on the spectrum: peaks from protons on the thymidine (T) ring are indicated by H, the ribose (R) protons are indicated by H′, and the GlcA (G) protons protons are indicated by H″. The peaks marked by an asterisk (*) are resonances from impurities.

B. cereus subsp. cytotoxis NVH 391-98 [19] motivated us to test the epimerase with UDP-GlcNAc and UDP-GlcNAcA as substrates, although no conversion was observed. However, the fact that the recombinant dehydrogenase (described above) was capable of utilizing TDP-Glc prompted us to test whether TDP-GlcA could be utilized as a substrate. Indeed, the recombinant BcUGlcAE converted a portion of TDP-GlcA to a new product as observed after separation by HPLC (Fig. 5C, panels 2 and 3, arrow). To further validate the nature of this new TDP-sugar, the peak was collected and its mass was analyzed by MALDI-TOF MS and the structure by NMR. The major mass ion at *m/z* 577.6 suggested a TDP-hexuronic acid (Fig. 6A) and ^{1}H-NMR (Fig. 6B) confirmed the epimerase product as TDP-GalA.

Enzymatic characterization of UGlcDH and UGlcAE

The *B. cereus* UDP-glucose 6-dehydrogenase (BcUGlcDH) had the highest activity at a temperature of 42 °C (Table S1). Additionally, the dehydrogenase was found to have substantial activity at high pH with its optimal pH at 9.0 in sodium phosphate buffer (Table S1). Relatively little UDP-GlcA was produced in enzymatic assays conducted at pH 4 or lower. Optimal epimerase activity was observed at 55 °C and, similar to the dehydrogenase, it was also most active above pH 7. Epimerase assays conducted at pH 8.2 in sodium phosphate buffer yielded the highest levels of activity. Kinetic analyses of the enzymes are summarized in Table 1. The data from kinetic experiments of dehydrogenase with UDP-Glc as the variable substrate and NAD^+ as the fixed substrate (or *vice versa*) fit well to the Michaelis–Menten model. The apparent K_m value for the dehydrogenase utilizing UDP-Glc was 137.2 μM for UDP-Glc and 42.3 μM for NAD^+, with V_{max} values of 27.1 $pmol \cdot s^{-1}$. The k_{cat}/K_m ($mM^{-1} \cdot s^{-1}$) values for the dehydrogenase were found to be 7.1 (UDP-Glc) and 21.4 (NAD^+). When TDP-Glc was used as the substrate, the apparent K_m values for the dehydrogenase were 2067 μM (TDP-Glc) and 644 μM (NAD^+). The V_{max} was found to be 19.5 $pmol \cdot s^{-1}$ when TDP-Glc was the variable substrate and 9.26 $pmol \cdot s^{-1}$ when variable concentrations of NAD^+ were used, and the k_{cat}/K_m ($mM^{-1} \cdot s^{-1}$) values were 0.31 for TDP-Glc and 0.46 for NAD^+. The epimerase had apparent K_m values of 120 μM (UDP-GlcA) and 180 μM when TDP-GlcA was used as the substrate.

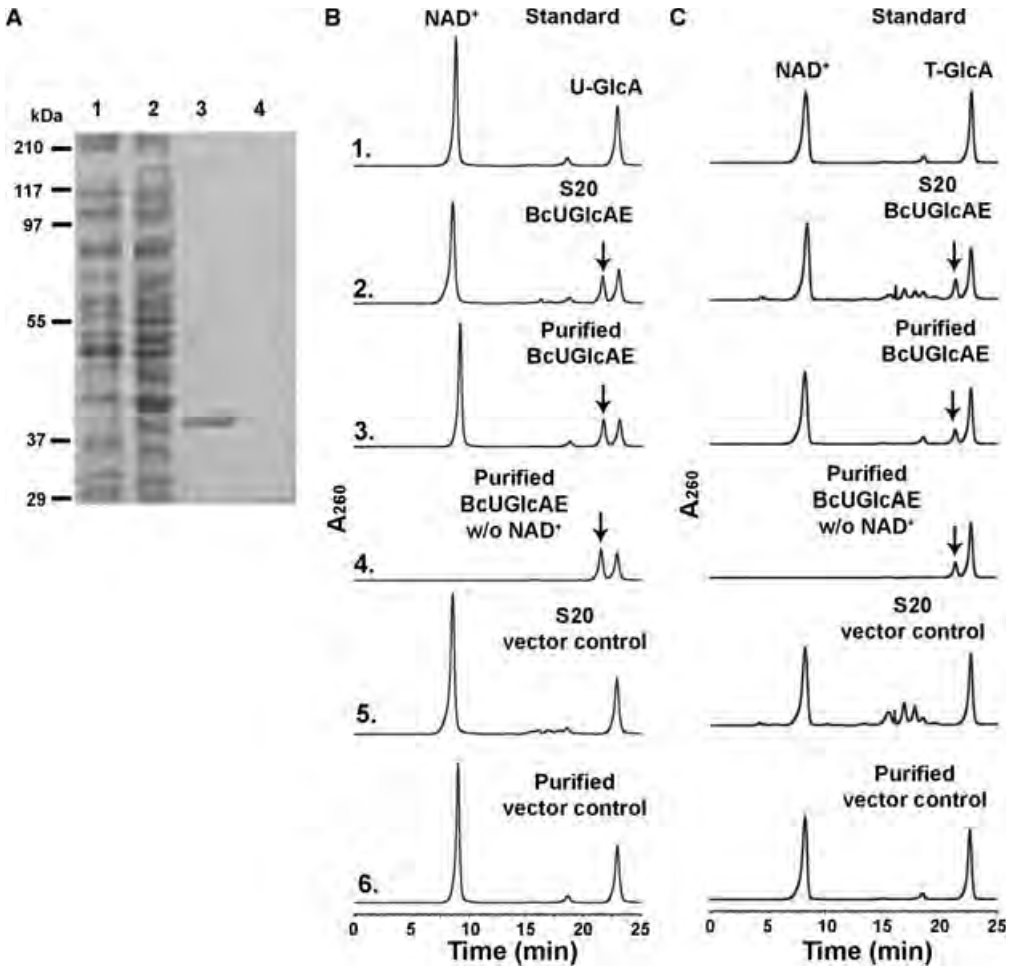

Fig. 5. Expression and characterization of recombinant BcUGlcAE. (A) SDS/PAGE of total soluble protein isolated from *E. coli* cells expressing BcUGlcAE (lane 1), control vector (lane 2) and of column-purified BcUGlcAE or control (lanes 3 and 4, respectively). (B) HPLC analysis of the products formed by BcUGlcAE reacting with UDP-GlcA. Total soluble proteins (denoted S20) or purified recombinant UGlcAE was reacted with UDP-GlcA for 30 min in the presence (panels 2 and 3), or absence (panel 4) of NAD^+. The crude or purified protein isolated from cells expressing control vector was incubated with UDP-GlcA for 60 min (panels 5 and 6) as a control. The distinct UDP-sugar peak marked by the arrow (panels 2–4 with the same retention time) was collected and analyzed by ^{1}H-NMR spectroscopy. (C) HPLC analysis of BcUGlcAE reacted with TDP-GlcA to yield a product (marked by an arrow in panels 2–4) that was collected and analyzed by NMR and MALDI-TOF.

The k_{cat}/K_m ($mM^{-1}\cdot s^{-1}$) values were 26 (UDP-GlcA) and 12 (TDP-GlcA). Inhibition studies (Tables S2 and S3) have shown that the *Bacillus* dehydrogenase is strongly inhibited by its product NADH, whereas, on the other hand, NADH had only a marginal inhibitory effect on the epimerase activity. However, the epimerase was highly inhibited by UDP and to a lesser extent by UDP-xylose.

Size-exclusion chromatography analysis of the epimerase gave an estimated molecular mass of 46.5 kDa, suggesting that the BcUGlcAE is active in a monomeric form (Table S1). Active dehydrogenase eluted from the size-exclusion column (Table S1) consistently with two distinctive peaks of activity: the first (with $\sim$ 20% of total activity) corresponded to a molecular mass of 152.1 kDa and the second corresponded to a molecular mass of 80.8 kDa. Considering the theoretical molecular mass of the dehydrogenase (49 kDa) and the 2 : 1 ratio of the estimated masses for the two active forms of the enzyme, size-exclusion chromatography suggested that the enzyme was most likely active as a monomer. Performing the size-exclusion chromatography of the dehydrogenase in the presence of UDP, UDP-Glc and NAD^+, or only with NADH, yielded the same elution pattern (data not shown). The elution behavior of the dehydrogenase from the

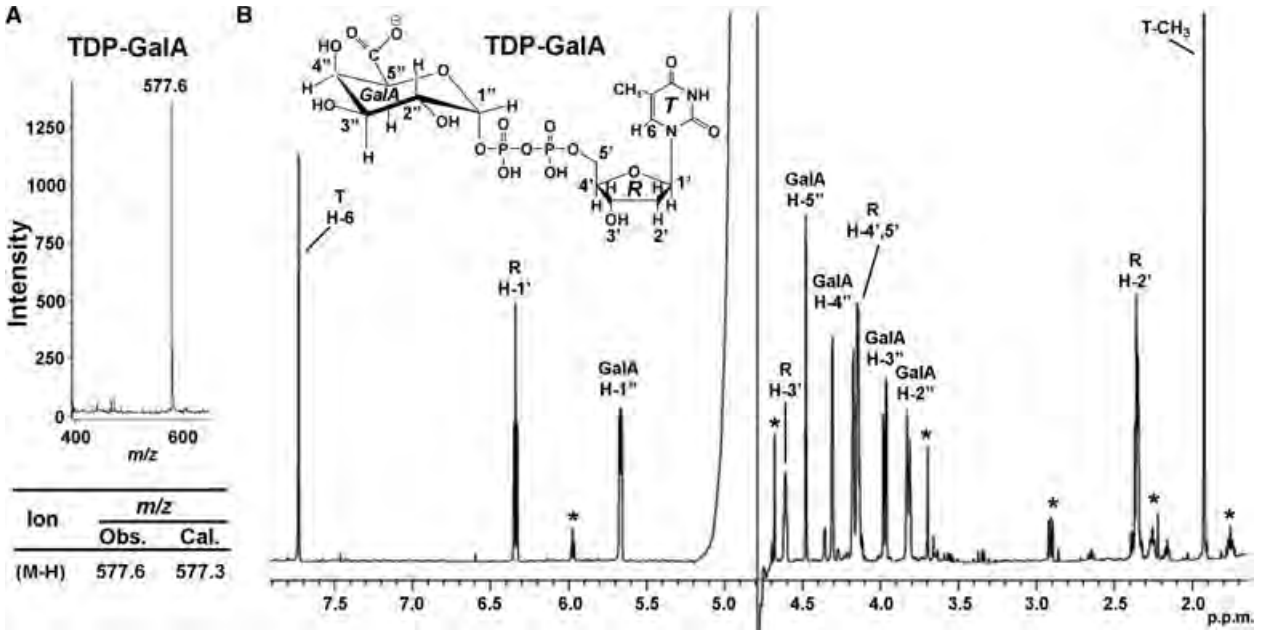

Fig. 6. ^{1}H-NMR spectroscopic and MALDI-TOF analyses of BcUGlcAE reaction products indicates the formation of TDP-α-D-galacturonic acid. (A) The HPLC peaks (Fig. 5C, panels 2–4) corresponding to the product formed by BcUGlcAE were collected and analyzed by MALDI-TOF. (B) ^{1}H-NMR spectroscopy at 600 MHz of the HPLC peak from Fig. 5C (panel 3). The assignments of each proton are indicated on the spectrum: peaks from protons on the thymidine (T) ring are indicated by H, the ribose (R) protons are indicated by H′, and the GalA (G) protons protons are indicated by H″. The peaks marked by an asterisk (*) are resonances from impurities.

column is not sufficient to draw conclusion for its size. It could be function as a monomer or as a dimer and efforts to crystalize the dehydrogenase are in progress aiming to determine its form(s) in solution.

Discussion

In the present study, we have demonstrated that the food borne pathogenic bacterium *B. cereus* subsp. cytotoxis NVH 391-98 contains an operon that functions to generate acidic sugar- precursors (UDP-GlcA, UDP-GalA and possibly their TDP-analogs). The operon organization (Bcer98_2076, Bcer98_2077, Bcer98_2079) is conserved in few terrestrial *Bacillus* spp. including *B. weihenstephanensis* KBAB4, *B. thuringiensis* IBL 200, *Geobacillus* sp. G11MC16, and *B. subtilis* subsp. subtilis str. 168. Similar genes are also found in sea-dwelling bacteria such as *Bacillus halodurans* C-125 and others, although the operon organization varies slightly.

The UGalA operon also contains a putative glycosyltransferase, which may utilize the UDP-GlcA and/or UDP-GalA as substrates for the biosynthesis of acidic sugar-containing glycans (e.g. the acidic glycan secreted by *B. cereus* living in biofilm). Glycans containing GlcA and GalA have been also noted in the cell walls of alkaliphilic *Bacillus* species *B. halodurans* C-125 and *Oceanobacillus iheyensis*. The amount of polymers containing these acidic sugars increases when such *Bacillus* spp. are grown in an alkaline environment. It has been demonstrated that alkaline conditions (up to pH 9) do not substantially inhibit the growth of *B. cereus* [20,21], and certain *Bacillus* spp., such as the deep sea-dwelling *O. iheyensis*, can grow at pH 10 [22]. It has been hypothesized that the presence of these acidic sugars in the outer layers of the cell wall serves to permit growth in an alkaline pH [23,24]. The enzymatic activity of the dehydrogenase (Fig. 1A) could also help to promote survival in high pH environments because three moles protons are released per mole of UDP-GlcA formed: two protons are released to form NADH, and, at a pH of the cytosolic environment above 3.8, the carboxylic moiety of UDP-GlcA is deprotonated. Oxidation of the produced NADH could further generate free protons for the cell. An additional mechanism that may facilitate growth at high pH is the fact that a number of *Bacillus* spp. produce 'pectinases' and 'lyases' under alkaline conditions. Such hydrolytic enzymes are capable of hydrolyzing polygalacturonan [25] and perhaps the cell's own uronic-acid glycan. Such enzymes from *B. cereus*, *B. subtilis* and *Bacillus* sp. BP-23, for example, have been found

to be optimally active at pH 8.5, 9.5 and 10, respectively [26,27]. Genes for the transport and catabolism of GlcA and GalA have been identified in *Bacillus* spp., and the release of these free acidic sugars may help to permit *Bacillus* spp. growth in alkaline environments [28]. At high pH, *Bacillus* spp. can hydrolyze polyanionic oligosaccharide structures (i.e. GlcA- and GalA-containing glycans) and the free acidic sugars can be transported to the cell where GlcA and GalA metabolites can serve as a source of protons to acidify the cytoplasm despite the high external pH.

The balance between the oxidized and reduced forms of NAD^+ is assumed to reflect the metabolic activities of the cell, and the fact that the recombinant *B. cereus* dehydrogenase is strongly inhibited in the presence of NADH may point to the role of the UGalA operon in the *B. cereus* lifecycle. It is possible that the dehydrogenase serves as a checkpoint in the regulation of downstream metabolic pathways utilizing UDP-GlcA or UDP-GalA because high NADH levels will likely strongly inhibit UDP-GlcA formation and therefore also hinder UDP-GalA production *in vivo*. This suggests that *B. cereus*, in a state of abundant intracellular energy (i.e. a high NADH/NAD^+ ratio), may produce less GlcA and/or GalA-containing glycans. On the other hand, one function of the dehydrogenase could be to support the formation of NADH for various metabolic pathways, especially under conditions when the bacterium is deprived of essential nutrients and required to form a protective spore. This may reflect a possible role of the operon in the biosynthesis of GlcA and GalA-containing glycans in a nutrient-starved cell (e.g. during sporulation). The intracellular concentration of NADH may act to modulate UDP-GlcA and UDP-GalA production in vegetative cells. Indeed, NADH inhibition may be a conserved feature of some UGlcDHs and has been reported in spore and nonspore forming bacteria alike. For example, NADH has been shown to inhibit a UGlcDH (TuaD BSU35580) of *B. subtilis* subsp. 168 that is distinct from the BcUGlcDH homolog, as well as UGlcDHs from *P. aeruginosa* PAO1 [29] and *Cryptococcus neoformans* [30].

The enzyme specificity and the nature of their evolution are fundamental questions with respect to bacterial UGlcAE. For example, the *K. pneumoniae* UGlcAE can 4-epimerize UDP-GlcA, UDP-Glc and UDP-GlcNAc, whereas the *Bacillus* enzyme has a strict specificity for the uronic acid moiety. The Cap1J UGlcAE from *S. pneumoniae* has also been shown to have specificity for the uronic acid moiety, and is capable of 4-epimerizing UDP-GlcA and UDP-GalA at the same time as being unable to interconvert UDP-Glc and UDP-Gal; unfortunately, whether Cap1J can utilize UDP-GlcNAc, UDP-GlcNAcA or other nucleotide sugars has not been tested [16]. We have tried to address the promiscuity of some 4-epimerases by analyzing the origin of UGlcAE proteins (from the known UGlcAE and homologs that share high amino acid sequence identity). Phylogenic analysis of eukaryotic and bacterial UGlcAE clearly separates the *Bacillus* spp. UGlcAE into a separate and distinct clade (Fig. S2A). Although plant and promiscuous bacterial UGlcAE are related (e.g. AtUGlcAE2, Cap1J and Gla_{kp}), the *Bacillus* spp. appear to belong to a different group that is well separated from other bacterial and eukaryotic UGlcAE. The phylogeny suggests that UGlcAE enzymes might share the same ancestor because those enzymes are well divided from UDP-glucose-4-epimerases (UGEs) and decarboxylases. However, currently we cannot predict the evolution of *Bacillus* UGlcAE.

The ability of the *Bacillus* dehydrogenase and epimerase to utilize TDP-Glc and TDP-GlcA, respectively, may point to a separate or additional role of the operon in the *B. cereus* life cycle. TDP-Glc is a product formed in *B. anthracis* for the synthesis of TDP-rhamnose (Rha) [31], and homologous proteins for TDP-Rha production are also found in the *B. cereus* genome [32]. In *B. anthracis*, Rha residues are incorporated into the spore glycoprotein bclA, and Rha residues have been shown to be major components of the glycans in the exosporium of *B. cereus* [33]. Rha is also a minor constituent of the biofilm exo-polysaccharides of *B. cereus* [7]. However, the capability of the enzymes to interconvert TDP-Glc and TDP-GlcA may be the result of the structural similarity between the thymine and uracil moieties of the TDP- and UDP-sugars.

At present, the function of glucuronic and galacturonic acid at different points of the *B. cereus* lifecycle remains to be determined, and the identification of the UGalA operon will help to allow the elucidation of their importance. Our laboratory is unfortunately not licensed to work with this human pathogen, as is necessary for genetic deletion of the operon; however, gene knockouts in nonpathogenic *Bacillus* spp. also possessing the UGalA operon (Fig. 1B) could be used to reveal its role. Efforts are underway to examine the function of these genes and perhaps their utilization in adapting to high pH in different *Bacillus* spp. Determination of the expression of the genes of the UGalA operon in response to various environment stimuli (e.g. alkaline pH, nutrient limitation or temperature extremes) may also be advantageous in developing an understanding of the biological role of the operon.

If the GalA-containing glycans are shown to be necessary for survival of the organism, the *Bacillus* UGlcAE may prove to be a potential target for drugs

combating this pathogen. As far as we are aware, humans do not synthesize GalA-containing glycans and are not considered to possess UGlcAEs. Indeed, the specificity of the *Bacillus* enzyme may permit the development of inhibitors restricted to BcUGlcAE that do not affect similar enzymes necessary for normal human metabolism.

Materials and methods

Cloning of BcUGlcDH and BcUGlcAE

The Bcer98_2076 and Bcer98_2077 genes from *Bacillus cereus* subsp. cytotoxis NVH 391-98, herein named, UDP-Glc 6-dehydrogenase (*BcUGlcDH*) and UDP-glucuronic acid 4-epimerase (*BcUGlcAE*), respectively, were cloned by high-fidelity PCR from genomic DNA. PCR primers were: sense 5′-Ccatggtgaatatatgcattataggatctg-3′ and antisense 5′-AAGCTTtgagcgaccaactcctacatagc-3′ for *BcUGlcDH*; and sense 5′-Tcatgaaaatacttgttactggagcag-3′ and antisense 5′-AAGCTTatataattgcttcatatactc-3′ for *BcUGlcAE*. Genomic DNA was kindly provided by the laboratory of A. Sorokin (Génétique Microbienne, INRA, France). The agarose gel-purified PCR fragments were cloned to yield the plasmids: pCR4-gmdh#2 and pCR4-gmad#1, respectively. The corresponding DNA sequences were deposited in Genbank (with respective accession numbers HM581980 and HM581979). The *Nco*1-*Hind*III fragment of *BcUGlcDH* (1289 bp) and *Bsp*H1-*Hind*III fragment of *BcUGlcAE* (944 bp) were cloned into an *E. coli* expression vector to form pET28b:BcUGlcDH#1 and pET28b:BcUGlcAE#1, respectively. The recombinant enzymes were designed to have a six-histidine extension at their C-terminus to facilitate affinity-purification.

Expression and purification of recombinant proteins

E. coli cells harboring pET28b:BcUGlcAE#1 or a control vector (pET28) were cultured for 16 h at 37 °C (or 30 °C for pET28b:BcUGlcDH#1 or a control vector) in 20 mL of LB medium supplemented with kanamycin (50 $\mu g \cdot mL^{-1}$) and chloramphenicol (34 $\mu g \cdot mL^{-1}$). A portion (5–7 mL) of the cultured cells was transferred into fresh LB liquid medium (250 mL) supplemented with the same antibiotics, and the cells were grown on a rotary shaker at 37 °C (BcUGlcAE) or 30 °C (BcUGlcDH) at 250 r.p.m. until D_{600} of 0.8 (BcUGlcAE) or 0.6 (BcUGlcDH) was reached. Isopropyl thio-β-D-galactoside (0.5 mM) was added to induce gene expression. The cells harboring pET28b:BcUGlcDH#1 were transferred to an incubator at 18 °C and grown for 20–24 h with shaking at 250 r.p.m.; cell harboring pET28b:BcUGlcAE#1 were incubated at 30 °C and grown for 4 h at 250 r.p.m. After induction, the cells were harvested by centrifugation (6000 ***g*** for 10 min at 4 °C) and suspended in 20 mL of lysis buffer. [For the dehydrogenase, the buffer was 50 mM Tris–HCl, pH 8, 20% glycerol (v/v), 1 mM EDTA, 100 mM NaCl, 25 mM KCl, 25 mM $(NH_4)_2SO_4$ supplemented with fresh 5 mM dithiothreitol and 0.5 mM phenylmethylsulfonyl fluoride; for BcUGlcAE, the lysis buffer was 50 mM sodium phosphate, pH 7.6, containing 10% (v/v) glycerol, 1 mM EDTA, and fresh 1 mM dithiothreitol and 0.5 mM phenylmethylsulfonyl fluoride] Cells were lysed by sonication [34] and centrifuged (6000 ***g*** for 10 min at 4 °C). The supernatant was supplemented with fresh dithiothreitol (1 mM for BcUGlcAE, 10 mM for BcUGlcDH) and centrifuged again (30 min at 20 000 ***g***). The resulting supernatant (termed S20) was kept at –20 °C. His-tagged proteins were purified on a Ni-Sepharose fast-flow column (GE Healthcare Life Sciences, Piscataway, NJ, USA; 2 mL of resin packed in a polypropylene column; inner diameter 1 cm × 15 cm). The column was pre-equilibrated with loading buffer [For BcUGlcAE, 50 mM sodium phosphate (pH 7.6), 0.1 M NaCl; for BcUGlcDH, 50 mM sodium phosphate (pH 8), 0.3 M NaCl]. The bound BcUGlcAE-6His was eluted with the same buffer containing an increased amount of imidazole (0–250 mM). Similarly, the bound BcUGlcDH-6His was eluted from Ni-column with solution adjusted to pH 8, which was composed of 0.3 M NaCl, 50 mM sodium phosphate and imidazole (0–250 mM). The fraction containing BcUGlcAE activity, typically eluted with 250 mM imidazole, was supplemented with 1 mM dithiothreitol and 10% glycerol, and was dialyzed (6000–8000 molecular weight cut-off; Spectrum Laboratories, Inc., Rancho Dominguez, CA, USA) three times (twice for 30 min, and once for ~ 1 h), each time against 800 mL of cold dialysis buffer [50 mM sodium phosphate, pH 7.6, containing 0.1 M NaCl, 10% (v/v) glycerol, 1 mM dithiothreitol]. The protein after dialysis was divided into small aliquots, flash frozen in liquid nitrogen and stored at –80 °C. The Ni-column fraction containing UDP-GlcDH activity, typically eluted with 250 mM imidazole, was supplemented with 20% glycerol, divided into aliquots, flash frozen and kept at −80 °C. Proteins extracted from *E. coli* cells expressing the control vector were obtained using the same purification protocol and were used as controls in enzyme assays and SDS/PAGE analyses. Proteins concentration was determined using the Bradford reagent with BSA as standard. The native molecular weight of the dehydrogenase and the epimerase was estimated by size-exclusion chromatography using a Superdex-75 column (GE Healthcare) as described previously [34].

UGlcDH and UGlcAE enzyme assays, HPLC and product analyses by NMR

Standard UGlcDH reactions (final volume of 50 μL) contained 100 mM sodium phosphate (pH 8), 20 mM KCl, 1 mM NAD^+, 0.5 mM UDP-Glc and 1.1 μg of purified

recombinant BcUGlcDH. UGlcAE reactions (final volume of 50 μL) contained 50 mM sodium phosphate (pH 7.6), 1 mM NAD^+, 1 mM UDP-GlcA and 0.2 μg of purified recombinant BcUGlcAE. UGlcAE or UGlcDH reactions were kept for up to 15 or 30 min, respectively, at 37 °C, and then terminated (100 °C water bath for 45 s). Reaction products were extracted with chloroform and chromatographed [34] on a Q15 anion-exchange column (1 × 250 mm; Amersham Pharmacia, Piscataway, NJ, USA) using an Agilent 1200 Series HPLC system equipped with an autosampler, diode-array detector and CHEMSTATION software (Agilent Technologies Inc., Santa Clara, CA, USA). Nucleotides were detected by their UV absorbance and the maximum absorbance for UDP-sugars, NAD^+ and NADH was 261, 259 and 259/340 nm, respectively. The amount of product formed was determined using calibration curves of standard UDP-GlcA. The product formed by the specific reaction (eluted from Q-column) was collected, lyophilized, dissolved in 99.9% D_2O, and analyzed by ^{1}H-NMR spectroscopy [34]. TDP-Glc, UDP-Glc, NADH, NAD^+ were obtained from Sigma (St Louis, MO, USA).

Characterization of the recombinant enzymes

UGlcDH and UGlcAE activities were determined using different buffers, at different temperatures, and in the presence of selected cations or potential inhibitors. For optimal pH studies, solutions of recombinant BcUGlcDH or BcUGlcAE were first mixed in 100 mM of each individual buffer. Subsequently, NAD^+ (1 mM) and UDP-Glc (0.5 mM) were added to BcUGlcDH reactions, whereas 1 mM NAD^+ and UDP-GlcA were added to BcUGlcAE reactions. Assays were then carried out for 15 min (UGlcAE) or 30 min (UGlcDH) at 37 °C. Assays to determine the optimal temperature of recombinant BcUGlcDH or BcUGlcAE were similarly run under standard UGlcDH or UGlcAE reaction conditions and incubated at variable temperatures for 15 min (UGlcAE) or 30 min (UGlcDH) before termination. UGlcDH or UGlcAE inhibition assays were performed by first mixing the enzyme with 100 mM phosphate buffer (pH 8) or 50 mM phosphate buffer (pH 7.6), respectively, with various additives (e.g. nucleotides) on ice for 10 min. UDP-Glc and NAD^+ (0.5 and 1 mM, respectively) were then added to UGlcDH assays, whereas 1 mM UDP-GlcA and NAD^+ were added to UGlcAE reactions. After 15 min (UGlcAE) or 30 min (UGlcDH) at 37 °C, the reactions were terminated and the amount of UDP-sugar formed was determined by quantitative-HPLC.

The steady-state kinetic experiments of BcUGlcAE were determined at 37 °C for 8 min in 50 mM sodium phosphate (pH 7.6), 1 mM NAD^+, with variable concentrations (0.1–1 mM) of UDP-GlcA (for UGlcAE activity), or with variable concentrations (0.08–0.50 mM) of TDP-GlcA (for TGlcAE activity), and 0.1 μg of purified protein. Steady-state kinetic of BcUGlcDH was similarly determined at 37 °C for 15 min in 0.1 M sodium phosphate buffer (pH 8), 20 mM KCl, and 1.5 μg of protein. When calculating the K_m for UDP-Glc or TDP-Glc, UGlcDH assays were carried out with fixed amount of NAD^+ (2 mM) and variable concentrations of UDP-Glc or TDP-Glc (0.1–1.0 mM); for the K_m value for NAD^+, BcUGlcDH was incubated with variable concentration of NAD^+ (0.1–2.0 mM) and a fixed amount of UDP-Glc or TDP-Glc (1 mM). DELTAGRAPH, version 5 (Red Rock Software, Inc., Salt Lake City, UT, USA) was used to generate a best-fit curve calculated by nonlinear regression analyses. The reciprocal initial velocity was plotted against the reciprocal nucleotide sugar concentration according to Lineweaver and Burk to calculate K_m values.

Acknowledgements

We thank Sung Lee and James A. Smith for technical help. This research was supported in part by NSF: IOB-0453664 (M.B.-P.) and by the BioEnergy Science Center (Grant DE-PS02-06ER64304), which is supported by the Office of Biological and Environmental Research in the DOE Office of Science. This research also benefited from activities at the Southeast Collaboratory for High-Field Biomolecular NMR, a research resource at the University of Georgia, funded by the National Institute of General Medical Sciences (NIGMS grant number GM66340) and the Georgia Research Alliance.

References

1 Leoff C, Saile E, Rauvolfova J, Quinn CP, Hoffmaster AR, Zhong W, Mehta AS, Boons GJ, Carlson RW & Kannenberg EL (2009) Secondary cell wall polysaccharides of Bacillus anthracis are antigens that contain specific epitopes which cross-react with three pathogenic Bacillus cereus strains that caused severe disease, and other epitopes common to all the Bacillus cereus strains tested. *Glycobiology* **19**, 665–673.

2 Raetz CR & Whitfield C (2002) Lipopolysaccharide endotoxins. *Annu Rev Biochem* **71**, 635–700.

3 Muszynski A, Laus M, Kijne JW & Carlson RW (2011) Structures of the lipopolysaccharides from *Rhizobium leguminosarum* RBL5523 and its UDP-glucose dehydrogenase mutant (exo5). *Glycobiology* **21**, 55–68.

4 Quelas JI, Mongiardini EJ, Casabuono A, Lopez-Garcia SL, Althabegoiti MJ, Covelli JM, Perez-Gimenez J, Couto A & Lodeiro AR (2010) Lack of galactose or galacturonic acid in *Bradyrhizobium japonicum* USDA 110 exopolysaccharide leads to different symbiotic responses in soybean. *Mol Plant-Microbe Interact: MPMI* **23**, 1592–1604.

5 Frirdich E & Whitfield C (2005) Characterization of Gla(KP), a UDP-galacturonic acid C4-epimerase from

Klebsiella pneumoniae with extended substrate specificity. *J Bacteriol* **187**, 4104–4115.
6 Arrecubieta C, Lopez R & Garcia E (1996) Type 3-specific synthase of *Streptococcus pneumoniae* (Cap3B) directs type 3 polysaccharide biosynthesis in *Escherichia coli* and in pneumococcal strains of different serotypes. *J Exp Med* **184**, 449–455.
7 Ratto M, Suihko ML & Siika-aho M (2005) Polysaccharide-producing bacteria isolated from paper machine slime deposits. *J Ind Microbiol Biotechnol* **32**, 109–114.
8 Slock JA & Stahly DP (1974) Polysaccharide that may serve as a carbon and energy storage compound for sporulation in *Bacillus cereus*. *J Bacteriol* **120**, 399–406.
9 Oh SY, Budzik JM, Garufi G & Schneewind O (2011) Two capsular polysaccharides enable *Bacillus cereus* G9241 to cause anthrax-like disease. *Mol Microbiol* **80**, 455–470.
10 Forsberg LS, Choudhury B, Leoff C, Marston CK, Hoffmaster AR, Saile E, Quinn CP, Kannenberg EL & Carlson RW (2011) Secondary cell wall polysaccharides from *Bacillus cereus* strains G9241, 03BB87, and 03BB102 causing fatal pneumonia share similar glycosyl structures with the polysaccharides from *Bacillus anthracis*. *Glycobiology* **21**, 934–948.
11 Bar-Peled M & O'Neill MA (2011) Plant nucleotide sugar formation, interconversion, and salvage by sugar recycling. *Annu Rev Plant Biol* **62**, 127–155.
12 Molhoj M, Verma R & Reiter WD (2004) The biosynthesis of D-galacturonate in plants. functional cloning and characterization of a membrane-anchored UDP-D-glucuronate 4-epimerase from *Arabidopsis*. *Plant Physiol* **135**, 1221–1230.
13 Gu X & Bar-Peled M (2004) The biosynthesis of UDP-galacturonic acid in plants. Functional cloning and characterization of Arabidopsis UDP-D-glucuronic acid 4-epimerase. *Plant Physiol* **136**, 4256–4264.
14 Gu X, Wages CJ, Davis KE, Guyett PJ & Bar-Peled M (2009) Enzymatic characterization and comparison of various poaceae UDP-GlcA 4-epimerase isoforms. *J Biochem* **146**, 527–534.
15 Smith EE, Mills GT, Bernheimer HP & Austrian R (1958) The presence of an uronic acid epimerase in a strain of pneumococcus type I. *Biochim Biophys Acta* **29**, 640–641.
16 Munoz R, Lopez R, de Frutos M & Garcia E (1999) First molecular characterization of a uridine diphosphate galacturonate 4-epimerase: an enzyme required for capsular biosynthesis in *Streptococcus pneumoniae* type 1. *Mol Microbiol* **31**, 703–713.
17 Kimmel JL & Tipton PA (2005) Inactivation of GDP-mannose dehydrogenase from *Pseudomonas aeruginosa* by penicillic acid identifies a critical active site loop. *Arch Biochem Biophys* **441**, 132–140.
18 Miller WL, Matewish MJ, McNally DJ, Ishiyama N, Anderson EM, Brewer D, Brisson JR, Berghuis AM & Lam JS (2008) Flagellin glycosylation in *Pseudomonas aeruginosa* PAK requires the O-antigen biosynthesis enzyme WbpO. *J Biol Chem* **283**, 3507–3518.
19 Gu X, Glushka J, Lee SG & Bar-Peled M (2010) Biosynthesis of a new UDP-sugar, UDP-2-acetamido-2-deoxyxylose, in the human pathogen *Bacillus cereus* subspecies cytotoxis NVH 391-98. *J Biol Chem* **285**, 24825–24833.
20 Raevuori M & Genigeorgis C (1975) Effect of pH and sodium chloride on growth of *Bacillus cereus* in laboratory media and certain foods. *Appl Microbiol* **29**, 68–73.
21 Valero M, Fernandez PS & Salmeron MC (2003) Influence of pH and temperature on growth of *Bacillus cereus* in vegetable substrates. *Int J Food Microbiol* **82**, 71–79.
22 Lu J, Nogi Y & Takami H (2001) *Oceanobacillus iheyensis* gen. nov., sp. nov., a deep-sea extremely halotolerant and alkaliphilic species isolated from a depth of 1050 m on the Iheya Ridge. *FEMS Microbiol Lett* **205**, 291–297.
23 Aono R & Uramoto M (1986) Presence of fucosamine in teichuronic acid of the alkalophilic *Bacillus* strain C-125. *Biochem J* **233**, 291–294.
24 Takami H, Takaki Y & Uchiyama I (2002) Genome sequence of *Oceanobacillus iheyensis* isolated from the Iheya Ridge and its unexpected adaptive capabilities to extreme environments. *Nucleic Acids Res* **30**, 3927–3935.
25 Namasivayam E, Ravindar J & Mariappan K (2011) Production of extracellular pectinase by *Bacillus cereus* isolated from market solid waste. *J Bioanal Biomed* **3**, 70–75.
26 Soriano M, Blanco A, Diaz P & Pastor FI (2000) An unusual pectate lyase from a *Bacillus* sp. with high activity on pectin: cloning and characterization. *Microbiology* **146**, 89–95.
27 Ahlawat S, Mandhan R, Dhiman SS, Kumar R & Sharma J (2008) Potential application of alkaline pectinase from *Bacillus subtilis* SS in pulp and paper industry. *Appl Biochem Biotechnol* **149**, 287–293.
28 Pujic P, Dervyn R, Sorokin A & Ehrlich SD (1998) The kdgRKAT operon of *Bacillus subtilis*: detection of the transcript and regulation by the kdgR and ccpA genes. *Microbiology* **144**, 3111–3118.
29 Hung RJ, Chien HS, Lin RZ, Lin CT, Vatsyayan J, Peng HL & Chang HY (2007) Comparative analysis of two UDP-glucose dehydrogenases in *Pseudomonas aeruginosa* PAO1. *J Biol Chem* **282**, 17738–17748.
30 Bar-Peled M, Griffith CL, Ory JJ & Doering TL (2004) Biosynthesis of UDP-GlcA, a key metabolite for capsular polysaccharide synthesis in the pathogenic fungus *Cryptococcus neoformans*. *Biochem J* **381**, 131–136.
31 Dong S, McPherson SA, Wang Y, Li M, Wang P, Turnbough CL Jr & Pritchard DG (2010) Characterization of the enzymes encoded by the anthrose

biosynthetic operon of *Bacillus anthracis*. *J Bacteriol* **192**, 5053–5062.
32 Graninger M, Kneidinger B, Bruno K, Scheberl A & Messner P (2002) Homologs of the Rml enzymes from *Salmonella enterica* are responsible for dTDP-beta-L-rhamnose biosynthesis in the gram-positive thermophile *Aneurinibacillus thermoaerophilus* DSM 10155. *Appl Environ Microbiol* **68**, 3708–3715.
33 Fox A, Black GE, Fox K & Rostovtseva S (1993) Determination of carbohydrate profiles of *Bacillus anthracis* and *Bacillus cereus* including identification of O-methyl methylpentoses by using gas chromatography-mass spectrometry. *J Clin Microbiol* **31**, 887–894.
34 Gu X, Glushka J, Yin Y, Xu Y, Denny T, Smith J, Jiang Y & Bar-Peled M (2010) Identification of a bifunctional UDP-4-keto-pentose/UDP-xylose synthase in the plant pathogenic bacterium *Ralstonia solanacearum* strain GMI1000, a distinct member of the 4,6-dehydratase and decarboxylase family. *J Biol Chem* **285**, 9030–9040.

Supporting information

The following supplementary material is available:
Fig. S1. Sequence comparison and phylogenic analysis of *Bacillus* UglcDH.
Fig. S2. Sequence comparison phylogenic analysis of *Bacillus* UGlcAE.
Table S1. Temperature and pH optima, and the estimated molecular mass estimated of BcUGlcAE and BcUGlcDH.
Table S2. The effects of NAD^+, NADH, $NADP^+$ and NADPH on BcUGlcDH activity.
Table S3. The effects of nucleotides and nucleotide sugars on BcUGlcAE activity.

This supplementary material can be found in the online version of this article.

Please note: As a service to our authors and readers, this journal provides supporting information supplied by the authors. Such materials are peer-reviewed and may be re-organized for online delivery, but are not copy-edited or typeset. Technical support issues arising from supporting information (other than missing files) should be addressed to the authors.